ACS OMEGA

http://pubs.acs.org/journal/acsodf

Article

# Solvent-Free Procedure to Prepare Ion Liquid-Immobilized Gel Polymer Electrolytes Containing $Li_{0.33}La_{0.56}TiO_3$ with High Performance for Lithium-Ion Batteries

Wen Zheng, Wanying Bi, Yaobing Fang, Shuya Chang, Wenhui Yuan,* and Li Li

Cite This: *ACS Omega* 2021, 6, 25329−25337

Read Online

ACCESS | Metrics & More | Article Recommendations

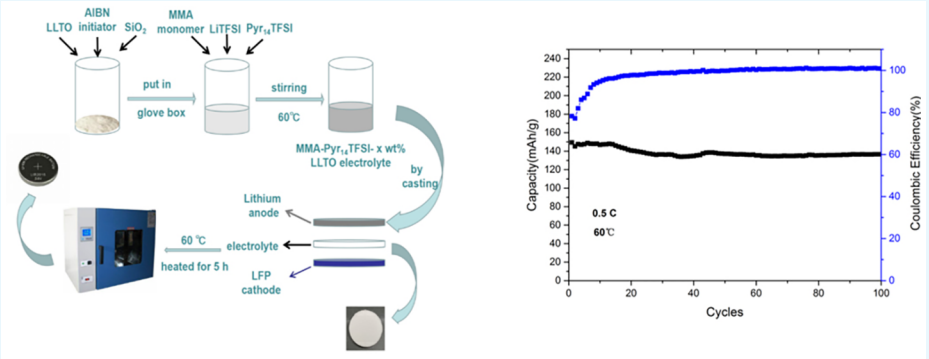


**ABSTRACT:** Based on the advantages of intrinsic safety, flexibility, and good interfacial contact with electrodes, a gel polymer electrolyte (GPE) is a promising electrolyte for lithium-ion batteries, compared with the conventional liquid electrolyte. However, the unstable electrochemical performance and the liquid state in a microscale limit the commercial application of GPE. Herein, we developed a novel gel polymer electrolyte for lithium-ion batteries by blending methyl methacrylate (MMA), *N*-butyl-*N*-methyl-piperidinium ($Pyr_{14}TFSI$), and lithium salts in a solvent-free procedure, with $SiO_2$ and $Li_{0.33}La_{0.56}TiO_3$ (LLTO) additives. The prepared MMA-$Pyr_{14}TFSI$-3 wt % LLTO electrolyte shows the best electrochemical performance and obtains a high ion conductivity of $4.51 \times 10^{-3}$ S $cm^{-1}$ at a temperature of 60 °C. Notably, the electrochemical window could be stable up to 5.0 V vs $Li^+/Li$. Moreover, the batteries with the GPE also show excellent electrochemical performance. In the $LiFePO_4$/MMA-$Pyr_{14}TFSI$-3 wt % LLTO/Li cell, a high initial discharge capacity was achieved 150 mA h $g^{-1}$ at 0.5C with a Coulombic efficiency over 99% and maintaining a good capacity retention of 90.7% after 100 cycles at 0.5C under 60 °C. In addition, the physical properties of the GPE have been investigated by scanning electron microscopy (SEM), X-ray diffraction (XRD) measurements, Fourier transform infrared (FTIR) spectroscopy, and thermogravimetry (TG).

## 1. INTRODUCTION

With the excessive consumption of fossil fuels, the demand for developing high-energy-density storage is urgent. Owing to the high operating voltage, memoryless effect, and excellent stability, lithium-ion batteries (LIBs) have been commonly applied in portable electric devices and electronic vehicles during the past decades and play a dominant role in the electronics market.[1−3] However, the growth of lithium dendrites and the flammable organic electrolyte has caused a concern for the security of electric vehicles using LIBs.[4−6] For example, the well-known explosion and ignition of a Samsung mobile phone and the Tesla car caused by unsafe lithium-ion batteries.[7−9] Therefore, to solve these troublesome safety issues, it is necessary to develop a novel electrolyte system to replace the conventional organic liquid electrolyte, and solid electrolyte could be a desirable alternative.[10,11]

Generally, solid-state LIBs show better safety due to the advantage that a solid-state electrolyte could intrinsically solve the problems of flammability, leakage, and short-circuiting of the battery caused by a lithium dendrite-piercing diaphragm compared with a conventional liquid-state electrolyte.[12−14] Unfortunately, a solid electrolyte always exhibits a low ion conductivity of about $10^{-7}$−$10^{-5}$ S $cm^{-1}$, which could not meet the demand of the practical application. A gel polymer electrolyte (GPE), consisting of a polymer matrix, lithium salts,

Received: June 15, 2021
Accepted: September 8, 2021
Published: September 21, 2021

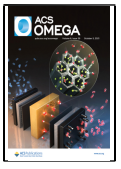

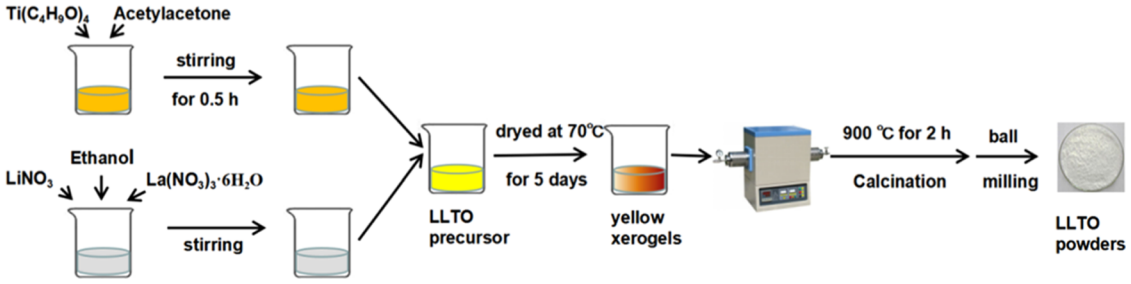


**Figure 1.** Schematic diagram of the preparation route of LLTO powders.

and a plasticizer, shows a high ionic conductivity of $10^{-3}$ S $cm^{-1}$ at ambient temperature, good compatibility between the electrolyte and electrodes, as well as a long service life. GPE combines the advantages of both solid and liquid electrolytes and possesses high ion conductivity and good mechanical properties.[15−18] However, the preparation of GPE is usually by the methods of immersing an electrolyte membrane into an organic liquid electrolyte or compounding the organic liquids and the polymer matrix, leading to the fact that a large amount of organic liquid still remains in the electrolyte, indicating that the abovementioned GPE has not yet satisfied the safety standards. Therefore, potential flammability and explosion still exist, and the organic solvents are also harmful to the environment. In addition, the increase in ion conductivity of GPE is always accompanied by a decrease in mechanical performance. In brief, an ideal gel polymer electrolyte applied in LIBs should have the properties of high ion conductivity, sufficient safety, and good electrochemical performance.[19−23]

Various strategies have been implemented to improve these properties; there are three main methods, which include copolymerization, blending, cross-link, and so forth; the addition of ceramic fillers; and the plasticizer additives.[24−27] The introduction of ceramic fillers into the polymer matrix not only improves the ion conductivity but also strengthens the mechanical properties of GPE. The metallic oxides such as $Al_2O_3$, $SiO_2$, and $ZrO_2$ in nanosize are generally used as ceramic particles in a polymer electrolyte, which could reduce the crystallization of the polymer matrix and further enhance the ion conductivity of the polymer electrolyte.[28−30] Pradeepa and co-workers[31] fabricated a composite polymer electrolyte based on poly(vinyl chloride)/poly(ethyl methacrylate) (PVC/PEMA) with the addition of ceramic fillers of $TiO_2$, and the results show that the ion conductivity and thermal stability of the polymer electrolyte have been greatly improved due to the addition of metallic oxide fillers. Except for the introduction of oxide fillers into the polymer electrolyte, active conducting fillers like LLZO and LLTO have been the prevailing additives to improve the electrochemical performance and ion conductivity of the electrolyte recently. Zhu and co-workers[32] developed a PEO-based composite polymer electrolyte filled with $Li_{0.33}La_{0.557}TiO_3$ nanofibres, which exhibited a high conductivity of $2.4 \times 10^{-4}$ S $cm^{-1}$ and a wide electrochemical window of 5 V vs $Li^+/Li$.[33] Furthermore, Cha and co-workers[34] synthesized a stable composite solid polymer electrolyte composed of a PEO matrix, a PEGDME plasticizer, and $Li_7La_3Zr_2O_{12}$, which exhibits the highest ion conductivity of $4.7 \times 10^{-4}$ S $cm^{-1}$ at 60 °C.[35]

Room-temperature ionic liquids (RTILs) have attracted increasing attention due to high ion conductivity and nonflammability and could be the preferred plasticizer in the polymer electrolyte for LIBs.[36] Anuar and co-workers[37] prepared an electrolyte based on PEMA-$NH_4SO_3CF_3$ with butyl-trimethyl ammonium bis(trifluoromethylsulfonyl)imide ionic liquid (BMATFSI). The electrolyte shows a relatively enhanced ion conductivity of $10^{-4}$ S $cm^{-1}$, demonstrating that the introduction of ionic liquid could increase the ionic conductivity of the electrolyte.

Poly(methyl methacrylate) (PMMA) has been widely used as a polymer matrix of an electrolyte applied for LIBs because of the environmental friendliness, good processing capability, low cost, and excellent electrochemical stability.[38] In addition, the liquid polymer monomer methyl methacrylate (MMA) is beneficial to dissolve the lithium salts and other fillers in the electrolyte. Unfortunately, the practical application of PMMA has been limited by low thermal stability and low ion conductivity.

In this work, we develop a gel polymer electrolyte by dissolving lithium salts using MMA and *N*-butyl-*N*-methylpyrrolidinium bis((trifluoromethyl)sulfonyl)imide ionic liquid ($Pyr_{14}TFSI$), and with $SiO_2$ and LLTO as fillers, and AIBN as a polymer initiator. The electrolyte was assembled in an $LiFePO_4$/GPE/Li cell, and then the cell was kept in a blast air oven at 60 °C for 5 h to make the electrolyte fully polymerized. With the advantages of nonflammability, electrochemical stability, and high ion conductivity of ion liquids, it is a good choice when preparing the ion liquid-immobilized GPE. The LLTO powders and $SiO_2$ are added to enhance the electrochemical performance and physical properties of GPE with the crystalline phase down and promotion of lithium-ion migration. The whole preparation of the GPE is carried out in solvent-free conditions and the disappearance of organic solvents not only enhances the safety performance but is also environmentally friendly. The electrochemical performance, such as the ion conductivity, electrochemical window, and cycling performance, and the physical properties (morphology, thermal stability, and crystalline structure) of GPE were studied and the results were obtained.

## 2. EXPERIMENTAL SECTION

**2.1. Material.** Methyl methacrylate (MMA) was purchased from Sigma-Aldrich to prepare a gel polymer electrolyte. Azobisisobutyronitrile (AIBN) from Sigma-Aldrich was used to achieve the polymerization of MMA. *N*-Butyl-*N*-methylpyrrolidinium bis((trifluoromethyl)sulfonyl)imide ($Pyr_{14}TFSI$) was purchased from Lanzhou Institute of Chemical Physics (Lanzhou China). $LiNO_3$ (>99.99%), $La(NO_3)_3·6H_2O$ (>99.99%), and $Ti(OC_4H_9)_4$ (>99.0%) were all provided by Aladdin, and all of the chemicals were used without further purification. In addition, the bis-(trifluoromethane)sulfonimide lithium salt (LiTFSI) and Nano silica from Aladdin were dried at 80 °C under vacuum for 24 h.


https://doi.org/10.1021/acsomega.1c03140
ACS Omega 2021, 6, 25329−25337

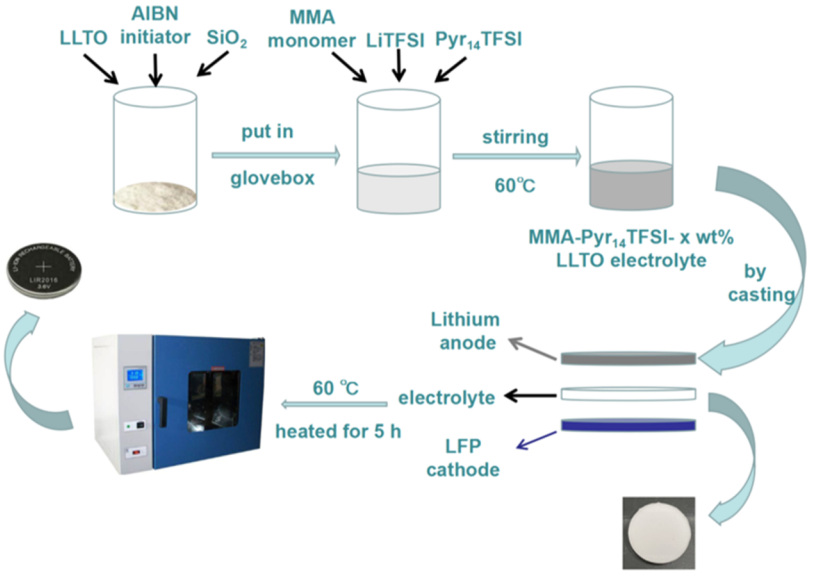


**Figure 2.** Schematic diagram of the preparation of the MMA-$Pyr_{14}TFSI$-*x* wt % LLTO electrolyte and the Li/GPE/LFP cell.

The syntheses of LLTO powders were accomplished by blending and calcination reported in the previous literature.[39] As shown in Figure 1, first, $LiNO_3$ and $La(NO_3)_3{\cdot}6H_2O$ were dissolved in ethanol with a mass ratio of 1:6 by vigorous stirring for 0.5 h to get a homogeneous and transparent solution. Meanwhile, acetylacetone and $Ti(OC_4H_9)_4$ were mixed with a fixed mass ratio of 3:1 by magnetic stirring for 0.5 h to gain a homogeneous Khaki-colored liquid. Then, the abovementioned solutions were mixed together by intense magnetic stirring for 2 h and a light Khaki homogeneous solution was obtained. Second, after being dried at 70 °C in an air-dry oven for about 1 week and followed by being dried at 80 °C in a vacuum for 24 h, the uniform solution became a Khaki Xerogel. At last, the white LLTO powders were obtained by calcination (remaining at 900 °C for 2 h) and ball milling, and then kept in a glovebox for the next experiment.

**2.2. Preparation of the MMA/$Pyr_{14}TFSI$/LLTO Gel Polymer Electrolyte.** Owing to the reason of that the electrolyte is easily oxidized in the air, all of the experiments were carried out in a glovebox ($H_2O$ < 0.1 ppm, $O_2$ < 0.1 ppm). First, MMA and $Pyr_{14}TFSI$ were mixed together with a molar ratio of 0.8:1, and a transparent solution was obtained by magnetic stirring for a few minutes. Second, a certain amount of $SiO_2$ (10 wt %) and LLTO (1, 3, 5 wt %) powders were successively added into the abovementioned solution, respectively. Subsequently, the uniform solution was obtained by vigorous magnetic stirring for 0.5 h at 50 °C. Finally, AIBN was added into the abovementioned solution with a weight ratio of 1:10 with respect to the weight of MMA, which produced a homogeneous stiff solution after another 0.2 h of magnetic stirring at 50 °C. Consequently, the gel polymer electrolyte was successfully achieved. All of the preparation processes of the gel polymer electrolyte are shown in Figure 2.

**2.3. Assemblage of the Solid-State Cell.** The fabrication of the CR2032 coin cells was carried out in a Mikrouna glovebox, using $LiFePO_4$ as a cathode, with a Li foil as a counter electrode, and the prepared gel polymer electrolyte. Then, the cells were subsequently heated in a drum wind dryer at 60 °C for 5 h to obtain a completely polymerized electrolyte. The final obtained solid-state cells were kept in a glovebox for 2 h before testing, and the cells with the electrolyte without LLTO were assembled as a control.

**2.4. Characterization.** Scanning electron microscopy (SEM; Hitachi SU8220) was conducted to characterize the surface morphology of the electrolyte samples. The crystallization and the structure of the samples were monitored by X-ray diffraction (XRD) (Bruker D8 Advance diffractometer, Germany) measurements with Cu Ka radiation from 10 to 90°. A Fourier transform infrared spectrometer (FTIR) (Bruker VERTEX 33, Germany) was used to investigate the composition of the samples with a range from 4500 to 500 $cm^{-1}$. The thermal properties of gel polymer electrolytes were studied by thermogravimetry (Netzsch 209F3) from 30 to 600 °C in a nitrogen atmosphere, with a linear heating rate of 10 °C $min^{-1}$. Tensile tests were carried out using a universal testing machine (SHIMADZU, EZ-LX) at a cross-head speed of 12 mm $min^{-1}$.

The electrochemical performances of prepared batteries were tested using a Neware CT-4008 battery test system (Shenzhen, China) and a Gamry electrochemical workstation.

Electrochemical impedance spectroscopy (EIS) was investigated to evaluate the ion conductivity of the gel polymer electrolyte with different amounts of LLTO powders in the CR2032 coin batteries, which were assembled by sandwiching the gel polymer electrolyte between two stainless steel electrodes with a diameter of 14 mm. The EIS measurements mentioned above were tested in a frequency range from $10^{-1}$ to $10^5$ HZ with an applied voltage of 5 mV and at temperatures of 60 °C. Ion conductivity ($\sigma$) was calculated from eq 1

$$\sigma = \frac{D}{R \times S} \tag{1}$$

where $D$ (cm) is the thickness of the gel polymer electrolytes, $R(\Omega)$ is the bulk resistance value in the measurements of EIS, and $S$ is the surface area of the electrode.

The linear sweep voltammetry (LSV) with the coin cells consisting of Li/GPE/stainless steel was measured to study the electrochemical stability window of a gel polymer electrolyte filled with different contents of LLTO at a potential range of 2−8 V with a scan rate of 0.5 mV $s^{-1}$ at ambient temperature.


https://doi.org/10.1021/acsomega.1c03140
ACS Omega 2021, 6, 25329−25337

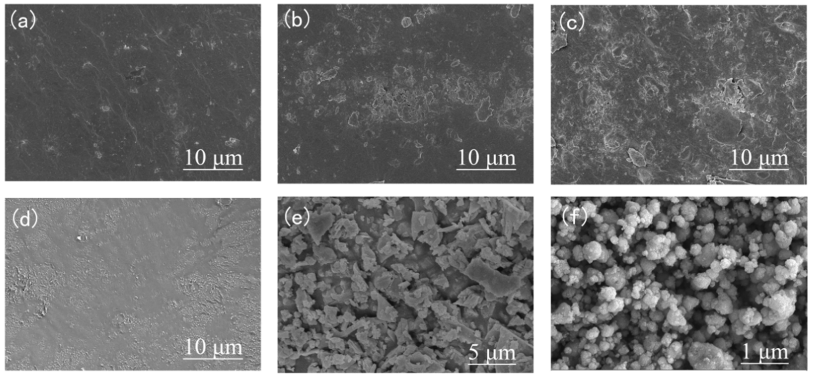


**Figure 3.** Surface morphologies of the gel polymer electrolyte: (a) MMA-$Pyr_{14}$TFSI-1 wt % LLTO, (b) MMA-$Pyr_{14}$TFSI-3 wt % LLTO, (c) MMA-$Pyr_{14}$TFSI-5 wt % LLTO, and (d) MMA-$Pyr_{14}$TFSI. The SEM images of LLTO: (e) before ball milling and (f) after ball milling.

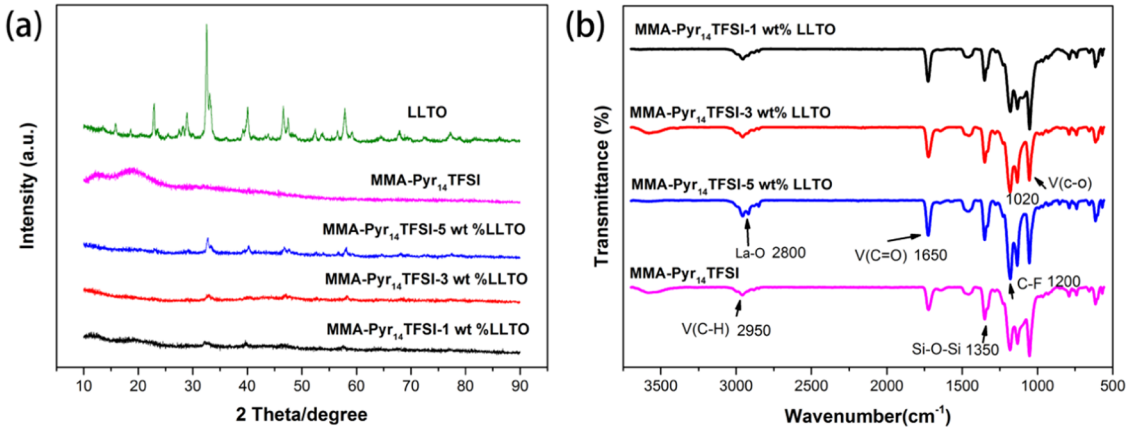


**Figure 4.** (a) XRD patterns of the gel polymer electrolytes based on MMA-$Pyr_{14}$TFSI with different contents of LLTO. (b) FTIR spectra of the MMA-$Pyr_{14}$TFSI-$x$ wt % LLTO electrolyte ($x$ = 1,3,5,0).

The galvanostatic charge/discharge stations were used to obtain the cycling and rate performance of the $LiFePO_4$/CPE/Li cells tested between 1.0 and 4.8 V at various current densities.

## 3. RESULTS AND DISCUSSION

### 3.1. Characterization of the Gel Polymer Electrolyte.

The morphology of the electrolyte film and the LLTO powders was characterized by SEM. As shown in Figure 3, it could be seen that the electrolyte film shows a dense and nonporous surface with some white powder (LLTO) attached. From Figure 3a–c, the LLTO with different contents are uniformly dispersed in the electrolyte film and increased in the film with the increasing contents of LLTO powders, compared with the electrolyte in Figure 3d, which shows a dense and nonporous film without white powders on it.

Figure 3e–f displays the morphology of the pristine LLTO and ball-milled LLTO. The LLTO exhibited a lump morphology before ball milling (Figure 3e), and the microsphere LLTO could be seen after ball milling (Figure 3f).

The characterization of XRD was carried out to investigate the crystal structures and chemical stability of the electrolyte samples. As shown in Figure 4a, it can be observed that the curves of MMA-$Pyr_{14}$TFSI-$x$ wt % LLTO polymer electrolytes show several diffraction peaks at 2$\theta$ values of 32, 40, and 58°, respectively, corresponding to the typical diffraction peaks of LLTO, indicating that LLTO has been successfully added into the gel polymer electrolyte and maintains the pristine structure well.

Moreover, with the increasing amount of LLTO in the electrolyte, the diffraction peaks of the MMA-$Pyr_{14}$TFSI-$x$ wt % LLTO electrolyte ($x$ = 1,3,5) show increasing intensity and no significant shift. Furthermore, the MMA-$Pyr_{14}$TFSI gel polymer electrolyte shows weak and wide diffraction peaks at a 2$\theta$ value of 19°, which could be attributed to the signals of the crystal phase of PMMA.[40] Compared with the curve of MMA-$Pyr_{14}$TFSI, the diffraction peaks at 19° almost disappear in the curves of the MMA-$Pyr_{14}$TFSI-$x$ wt % LLTO electrolyte ($x$ = 1,3,5) so that the addition of LLTO could decrease the crystallinity down in the gel polymer electrolyte, indicating more amorphous regions and increased ion conductivity of the electrolyte.

To further investigate the functional groups in the MMA-$Pyr_{14}$TFSI-$x$ wt % LLTO electrolyte ($x$ = 1,3,5,0), the FTIR spectrum analysis was performed. As shown in Figure 4b, the absorption peaks around 1020, 1200, and 1350 $cm^{-1}$ could be assigned to the stretching vibrations of C–O, C–F, and Si–O–Si, respectively.[41] The characteristic peak of C–H could be confirmed at 2950 $cm^{-1}$ and the characteristic group of La–O appears at 2800 $cm^{-1}$ due to the addition of LLTO, resulting in a new absorption peak of the La–O group, and the intensity of the peak increases with the increasing amount of LLTO.

Thermal stability is one of the most important factors of GPE, which could affect the electrochemical performance in LIBs. The TG and differential thermogravimetry (DTG)


https://doi.org/10.1021/acsomega.1c03140
ACS Omega 2021, 6, 25329–25337

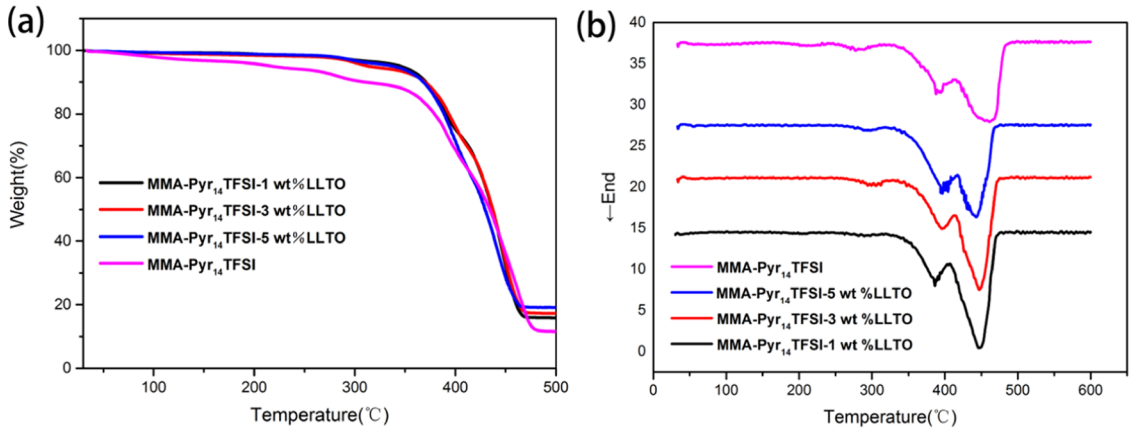


**Figure 5.** (a) TG curves and (b) DTG curves of gel polymer electrolytes with different contents of LLTO.

curves of MMA-$Pyr_{14}$TFSI-$x$ wt % LLTO ($x$ = 1,3,5,0) are shown in Figure 5a,b, respectively. It can be observed that the degradation of MMA-$Pyr_{14}$TFSI-$x$ wt % LLTO generally starts at about 360 °C, and the weight loss increases with the increasing temperature and the loss rate reached the highest value at almost 450 °C. While the degradation of MMA-$Pyr_{14}$TFSI starts at about 100 °C, its weight loss rate reached its maximum at about 460 °C. The residual weight of MMA-$Pyr_{14}$TFSI-$x$ wt % LLTO was about 42% at 450 °C. However, in the same condition, the residual weight of MMA-$Pyr_{14}$TFSI was about 35%, which is significantly lower than the above one, confirming that the MMA-$Pyr_{14}$TFSI-$x$ wt % LLTO shows better thermal stability than the pristine MMA-$Pyr_{14}$TFSI, indicating that the addition of LLTO enhances the thermal performance of the gel polymer electrolyte. The tensile strength has been tested and displayed in Figure 6. The

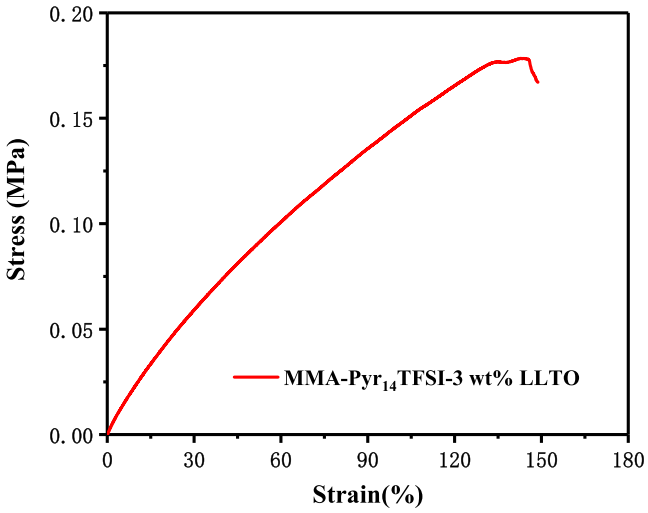


**Figure 6.** Stress−strain curves of the MMA-$Pyr_{14}$TFSI-3 wt % LLTO.

maximum stress of the MMA-$Pyr_{14}$TFSI-3 wt % LLTO gel polymer electrolyte is 0.18 MPa, which could reduce the possibility of lithium dendrite piercing and enhance the safety of LIBs.

**3.2. Electrochemical Performance of the $LiFePO_4$/GPE/Li Cell.** *3.2.1. Ionic Conductivity of Different Gel Polymer Electrolytes.* The ionic conductivity of the electrolyte plays a very important role in cell performance. Therefore, the electrochemical impedance spectroscopy (EIS) measurements were conducted to test the ionic conductivity of the GPE in an SS/GPE/SS cell.

Figure 7a displays the EIS spectra with the different gel polymer electrolytes, and it is obvious that the curves of the MMA-$Pyr_{14}$TFSI-$x$ wt % LLTO electrolyte ($x$ = 1,3,5) show lower bulk resistance than the curve of the pristine MMA-$Pyr_{14}$TFSI electrolyte, indicating that the ion conductivity of the MMA-$Pyr_{14}$TFSI-$x$ wt % LLTO electrolyte is much higher than the MMA-$Pyr_{14}$TFSI electrolyte, indicating that the addition of LLTO is beneficial to increase the ionic conductivity. In Table 1, the ionic conductivities of the gel polymer electrolyte with different contents of LLTO have been listed, and all of the tests were operated at a temperature of 60 °C. The MMA-$Pyr_{14}$TFSI-3 wt % LLTO electrolyte shows a high ionic conductivity of $4.51 \times 10^{-3}$ S $cm^{-1}$, higher than that of the MMA-$Pyr_{14}$TFSI-1 wt % LLTO electrolyte ($4.06 \times 10^{-3}$ S $cm^{-1}$) and the MMA-$Pyr_{14}$TFSI-5 wt % LLTO electrolyte ($8.1 \times 10^{-4}$ S $cm^{-1}$). The results show that 3 wt % LLTO could be an optimal ratio in a gel polymer electrolyte with ionic conductivity, which could be ascribed to the fact that the addition of a proper amount of LLTO could increase the segment motion of the gel polymer electrolyte but the excess of it could decrease the transport and motion of ions in electrolytes. Consequently, 3 wt % LLTO could be a proper ratio to obtain the highest ion conductivity of the gel polymer electrolyte.

*3.2.2. Electrochemical Stability of the Gel Polymer Electrolyte.* The electrochemical stability of the gel polymer electrolyte determines the operating voltage range of LIBs. Therefore, it is essential to widen the electrochemical stability window for the electrolyte.

To evaluate the electrochemical stability of different gel polymer electrolytes, linear sweep voltammetry (LSV) was conducted to investigate the electrochemical window of the gel polymer electrolyte in a Li/GPE/SS cell at ambient temperature.

As shown in Figure 7b, the MMA-$Pyr_{14}$TFSI-$x$ wt % LLTO electrolytes ($x$ = 1,3,5) exhibit a wide electrochemical stability window up to almost 4.8, 5.0, and 4.5 V, respectively, demonstrating that the gel polymer electrolytes with LLTO show good electrochemical stability. However, the LSV curve of the MMA-$Pyr_{14}$TFSI electrolyte shows a sudden increase at 4.5 V, indicating poor electrochemical stability, which means that the addition of LLTO could enhance the electrochemical stability of gel polymer electrolytes. In addition, the MMA-$Pyr_{14}$TFSI-3 wt % LLTO electrolyte showed the highest


https://doi.org/10.1021/acsomega.1c03140
ACS Omega 2021, 6, 25329−25337

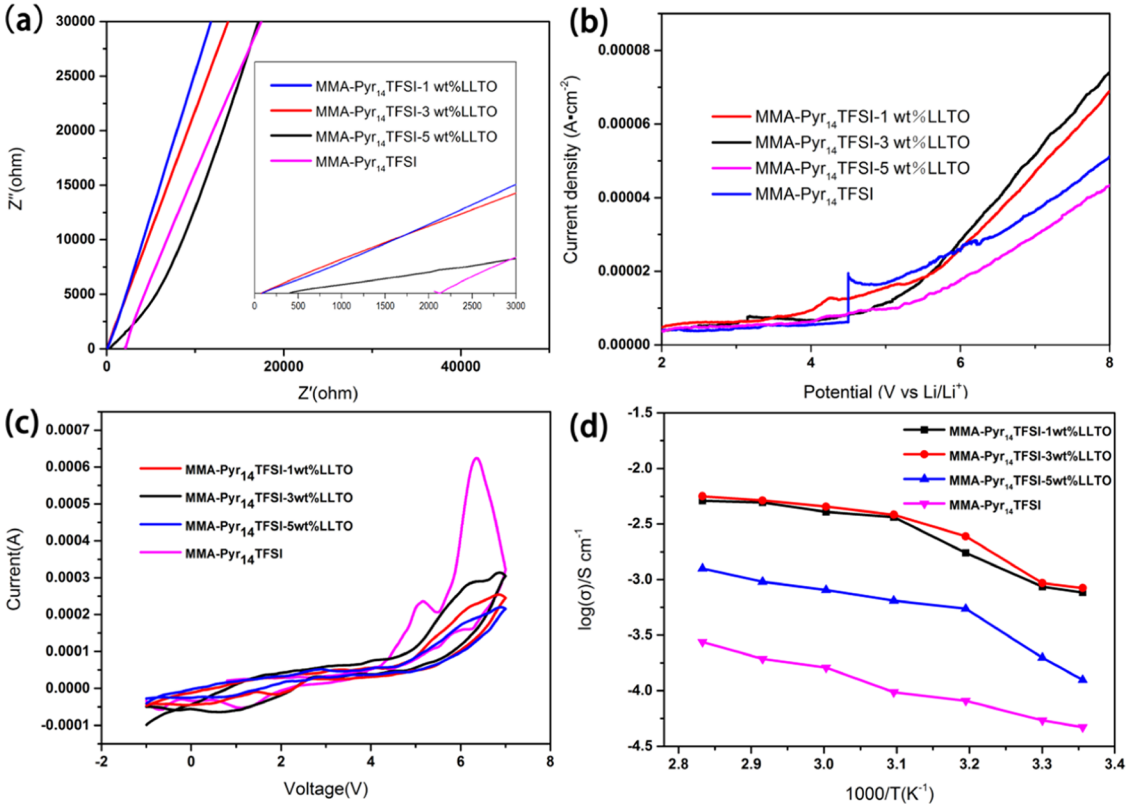


**Figure 7.** (a) EIS profile, (b) LSV curves of the MMA-$Pyr_{14}$TFSI gel polymer electrolyte with different contents of LLTO, (c) cyclic voltammogram of GPEs, and (d) Arrhenius plots of ionic conductivity vs temperature for the MMA-$Pyr_{14}$TFSI gel polymer electrolyte with different contents of LLTO.

**Table 1. Bulk Resistance and Ion Conductivity of the Gel Polymer Electrolyte Samples at 60 °C**

| sample | bulk resistance (Ω) | ion conductivity × $10^{-3}$ (S $cm^{-1}$) |
|---|---|---|
| MMA-$Pyr_{14}$TFSI-1 wt % LLTO | 82 | 4.06 |
| MMA-$Pyr_{14}$TFSI-3 wt % LLTO | 72 | 4.51 |
| MMA-$Pyr_{14}$TFSI-5 wt % LLTO | 402 | 0.81 |
| MMA-$Pyr_{14}$TFSI | 2020 | 0.16 |

electrochemical window up to 5.0 V vs $Li^+$/Li among all of the electrolyte samples, further indicating that 3 wt % LLTO is the most suitable ratio in gel polymer electrolytes. Furthermore, the cyclic voltammetry curves of GPEs are shown in Figure 7c, which is investigated at a scan rate of 0.3 mV $s^{-1}$. It could be noticed that there are a pair of cathodic and anodic peaks of each gel polymer electrolyte at around 3 V, which corresponds to the reduction and oxidation of lithium. Moreover, the gel polymer electrolytes with LLTO are more stable than the one without LLTO and all of the gel polymer electrolyte samples showed cathodic behavior at 0 V without the deposition process of lithium.

*3.2.3. Electrochemical Analysis of the Gel Polymer Electrolyte at Different Temperatures.* The temperature-dependent ionic conductivity of the gel polymer electrolyte has been measured via electrochemical impedance spectroscopy (EIS) at different temperatures, as shown in Figure 7d. The conductivity of the MMA-$Pyr_{14}$TFSI-3 wt % LLTO electrolyte is 5.16 × $10^{-3}$ S $cm^{-1}$ at 70 °C and 4.53 × $10^{-3}$ S $cm^{-1}$ at 60 °C, respectively, much higher than the conductivity at ambient temperature (8.42 × $10^{-4}$ S $cm^{-1}$). Obviously, the ionic conductivity values increase with the increased temperature, which could be ascribed to the gradually decreased bulk resistance and a reduced crystallization zone with increasing temperature, indicating that the high temperature could contribute to the migration of $Li^+$ and the movement of chain segments of the gel polymer electrolyte.

Moreover, the MMA-$Pyr_{14}$TFSI-3 wt % LLTO electrolyte and the MMA-$Pyr_{14}$TFSI-1 wt % LLTO electrolyte exhibit higher ionic conductivity at all temperatures than other gel polymer electrolytes, which may be attributed to the fact that the addition of moderate LLTO not only reinforces the lamellar structure but also increases the segment motion of the gel polymer electrolyte.

*3.2.4. Cycle Performance.* Figure 8a shows the typical discharge plots of Li/MMA-$Pyr_{14}$TFSI-3 wt % LLTO/$LiFePO_4$ cells with different cycles at a rate of 0.5C at 60 °C. In the first cycle, the battery shows a high discharge capacity (148 mA h $g^{-1}$), and after 100 cycles, the capacity is still maintained at 135 mA h $g^{-1}$, keeping a high capacity retention of 91.22%. Figure 8b exhibits the corresponding discharge−charge curves of the batteries with different amounts of LLTO at a temperature of 60 °C. It can be seen that the discharge specific capacities of the $LiFePO_4$/GPE/Li cell were 95, 109, 126, and 136 mA h $g^{-1}$ at 0.5C, respectively, and all of the batteries exhibit a well-defined and stable charge−discharge plateau, corresponding to the results of CV (Figure 6c).

The corresponding cycling performance of an MMA-$Pyr_{14}$TFSI-3 wt % LLTO electrolyte in a $LiFePO_4$/GPE/Li


https://doi.org/10.1021/acsomega.1c03140
ACS Omega 2021, 6, 25329−25337

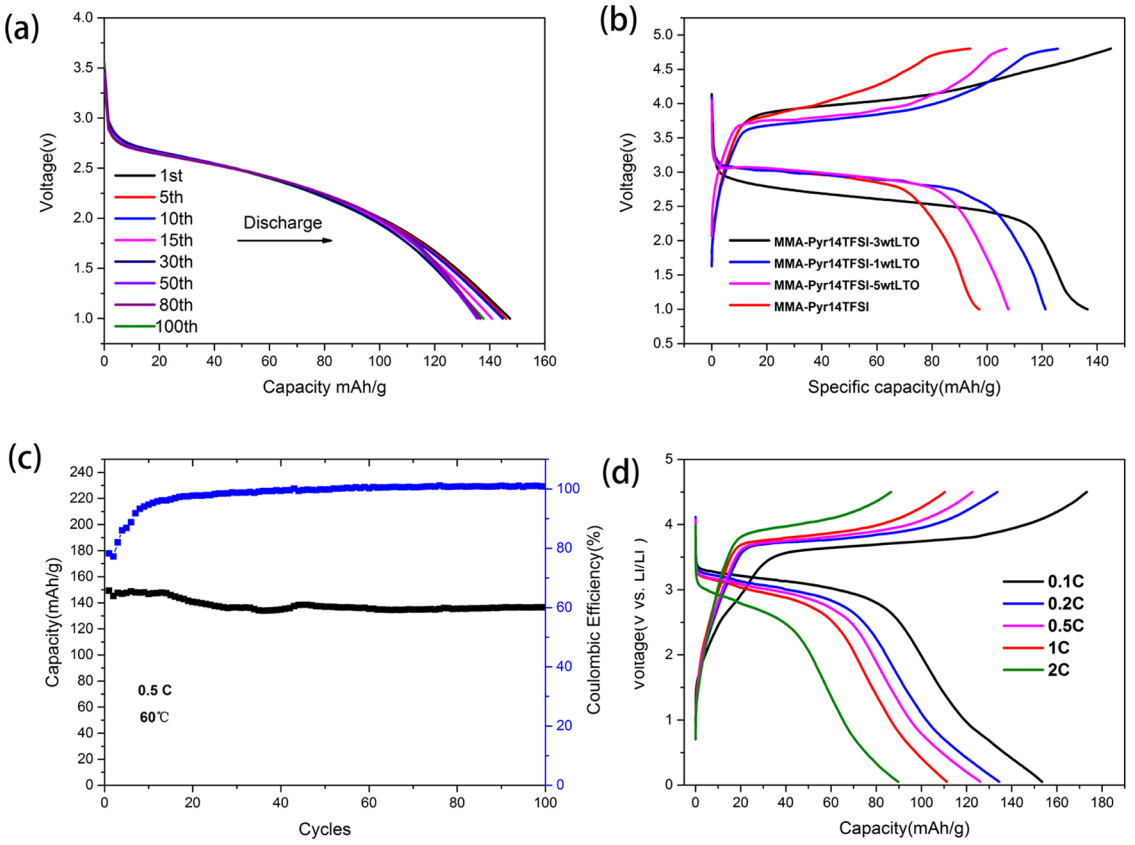


**Figure 8.** (a) Discharge curves of $LiFePO_4$/MMA-$Pyr_{14}$TFSI-3 wt % LLTO/Li at 0.5C and 60 °C at different cycles. (b) Charge and discharge curves of $LiFePO_4$/GPE/Li at 0.5C and 60 °C with four different kinds of electrolytes. (c) Long cycling performance of $LiFePO_4$/MMA-$Pyr_{14}$TFSI-3 wt % LLTO/Li at 0.5C and 60 °C. (d) Corresponding charge/discharge voltage curves at different rates.

cell is shown in Figure 8c. After the first seven cycles, the Coulombic efficiency is over 99%, and the capacity retention is maintained at 93.5% after 100 cycles, indicating an outstanding cycling performance, which is superior to the other gel polymer electrolyte reported in lithium-ion batteries;[42] the reason could be ascribed to the reinforced network of the gel polymer electrolyte by adding the LLTO powders and $SiO_2$ particles.[43] Figure 8d shows the charge and discharge curves of the MMA-$Pyr_{14}$TFSI-3 wt % LLTO electrolyte in the $LiFePO_4$/GPE/Li cell at different rates. With the increase in the current density, the discharge capacity decreases gradually caused by electrochemical polarization. The cell shows a high capacity (152 and 138 mA h·$g^{-1}$) at 0.1C and 0.2C, respectively. Moreover, the cell achieves a high discharge capacity (90 mA h $g^{-1}$) at high cycling rates (2C), demonstrating an excellent rate performance.

## 4. CONCLUSIONS

In summary, we fabricated a safe, high ion conductivity, good electrochemical performance gel polymer electrolyte in a solvent-free procedure. The physical properties and electrochemical performance of the prepared gel polymer electrolyte have been investigated comprehensively. The results demonstrate that LLTO could enhance the thermal and electrochemical performance, which could be ascribed to the fact that the addition of LLTO may reduce the crystallization and enhance the segment chain movement of a gel polymer electrolyte. In addition, 3 wt % LLTO has been demonstrated as an optimal ratio in an electrolyte, the GPE shows the highest conductivity of $4.54 \times 10^{-3}$ S $cm^{-1}$ at 60 °C, and the wide electrochemical window of the electrolyte is up to 5.0 V vs $Li^+$/Li. Moreover, the $LiFePO_4$/MMA-$Pyr_{14}$TFSI-3 wt % LLTO/Li cell shows good electrochemical performance, the highest discharge capacity could be achieved up to 148 mA h $g^{-1}$, and the capacity retention is maintained at 92% after 100 cycles with a Coulombic efficiency of 99.9%. In addition, the organic solvent-free procedure not only eliminates the liquid component in GPE but also decreases the harm of the organic liquid on the environment, indicating that the GPE and the unique process of LIBS could be veritably meaningful in the development of solid-state lithium batteries.

## AUTHOR INFORMATION


### Corresponding Author

**Wenhui Yuan** − *School of Chemistry and Chemical Engineering, South China University of Technology, Guangzhou 510640, China; Guangdong Engineering Technology Research Center of Advanced Insulating Coating, South China University of Technology-Zhuhai Institute of Modern Industrial Innovation, Zhuhai 519175, China;* orcid.org/0000-0002-8880-4542; Email: cewhyuan@scut.edu.cn

### Authors

**Wen Zheng** − *School of Chemistry and Chemical Engineering, South China University of Technology, Guangzhou 510640, China; Guangdong Engineering Technology Research Center of Advanced Insulating Coating, South China University of Technology-Zhuhai Institute of Modern Industrial Innovation, Zhuhai 519175, China*




https://doi.org/10.1021/acsomega.1c03140
*ACS Omega* 2021, 6, 25329−25337

**Wanying Bi** − *School of Chemistry and Chemical Engineering, South China University of Technology, Guangzhou 510640, China; Guangdong Engineering Technology Research Center of Advanced Insulating Coating, South China University of Technology-Zhuhai Institute of Modern Industrial Innovation, Zhuhai 519175, China*

**Yaobing Fang** − *School of Chemistry and Chemical Engineering, South China University of Technology, Guangzhou 510640, China; Guangdong Engineering Technology Research Center of Advanced Insulating Coating, South China University of Technology-Zhuhai Institute of Modern Industrial Innovation, Zhuhai 519175, China*

**Shuya Chang** − *School of Chemistry and Chemical Engineering, South China University of Technology, Guangzhou 510640, China; Guangdong Engineering Technology Research Center of Advanced Insulating Coating, South China University of Technology-Zhuhai Institute of Modern Industrial Innovation, Zhuhai 519175, China*

**Li Li** − *Guangdong Engineering Technology Research Center of Advanced Insulating Coating, South China University of Technology-Zhuhai Institute of Modern Industrial Innovation, Zhuhai 519175, China; School of Environment and Energy, South China University of Technology, Guangzhou 510006, China*

Complete contact information is available at: https://pubs.acs.org/10.1021/acsomega.1c03140

### Author Contributions

This manuscript was written through contributions of all authors. All authors have given approval to the final version of the manuscript.

### Notes

The authors declare no competing financial interest.

## ■ ACKNOWLEDGMENTS

This work was supported by the National Natural Science Foundation of China (No. 22075089) and the Project of Science and Technology of Jieyang City (No. 2019026, China).

## ■ REFERENCES

(1) Diao, C.; Dong, L.; Yang, Y.; Liu, H. Research Progress of Dielectric Energy Storage Thin Films and Methods for Improving Energy Storage Density. *Mater. Rep.* **2019**, *33*, 3921−3929.

(2) Tarascon, J. M.; Armand, M. Issues and Challenges Facing Rechargeable Lithium Batteries. *Nature* **2001**, *414*, 359−367.

(3) Scrosati, B.; Garche, J. Lithium Batteries: Status, Prospects and Future. *J. Power Sources* **2010**, *195*, 2419−2430.

(4) Wen, J.; Yu, Y.; Chen, C. A Review on Lithium-Ion Batteries Safety Issues: Existing Problems and Possible Solutions. *Mater. Express* **2012**, *2*, 197−212.

(5) Métivier, Y.; Richomme, G. On the Star Operation and the Finite Power Property in Free Partially Commutative Monoids. *Annu. Symp. Theor. Aspects Comput. Sci.* **1994**, 341−352.

(6) Zhang, J.; Zhang, L.; Sun, F.; Wang, Z. An Overview on Thermal Safety Issues of Lithium-Ion Batteries for Electric Vehicle Application. *IEEE Access* **2018**, *6*, 23848−23863.

(7) Dimas Caro, C. D.; Lopez, G. R.; Luna, A. C. *Fast Co-Simulation Methodology to Assess Electric Vehicle Penetration in Distribution Networks*, 2019 IEEE Industry Applications Society Annual Meeting. 2019, pp 1 5.

(8) Zhang, G.; Huang, F. *Research of the Electric Vehicle Safety Standard*, World Automation Congress Proceedings. 2012; Vol. 13, pp 8−11.

(9) Bashirpour-Bonab, H. Thermal Behavior of Lithium Batteries Used in Electric Vehicles Using Phase Change Materials. *Int. J. Energy Res.* **2020**, *44*, 12583−12591.

(10) Chen, S.; Wen, K.; Fan, J.; Bando, Y.; Golberg, D. Progress and Future Prospects of High-Voltage and High-Safety Electrolytes in Advanced Lithium Batteries: From Liquid to Solid Electrolytes. *J. Mater. Chem. A* **2018**, *6*, 11631−11663.

(11) Yada, C.; Brasse, C. Better Batteries With Solid-State Instead of Liquid-Based Electrolytes. *ATZelektronik Worldw.* **2014**, *9*, 10−15.

(12) Li, S.; Yang, K.; Zhang, Z.; Yang, L.; Hirano, S. I. Organic Ionic Plastic Crystal-Poly(Ethylene Oxide) Solid Polymer Electrolytes: Application in All-Solid-State Lithium Batteries. *Ind. Eng. Chem. Res.* **2018**, *57*, 13608−13614.

(13) Lyu, W.; He, G.; Liu, T. PEO-LITFSI-SiO2-SN System Promotes the Application of Polymer Electrolytes in All-Solid-State Lithium-Ion Batteries. *ChemistryOpen* **2020**, *9*, 713−718.

(14) Subramanian, K.; Alexander, G. V.; Karthik, K.; Patra, S.; Indu, M. S.; Sreejith, O. V.; Viswanathan, R.; Narayanasamy, J.; Murugan, R. A Brief Review of Recent Advances in Garnet Structured Solid Electrolyte Based Lithium Metal Batteries. *J. Energy Storage* **2021**, *13*, No. 102157.

(15) Song, J. Y.; Wang, Y. Y.; Wan, C. C. Review of Gel-Type Polymer Electrolytes for Lithium-Ion Batteries. *J. Power Sources* **1999**, *77*, 183−197.

(16) Yusuf, S. N. F.; Yusof, S. Z.; Kufian, M. Z.; Teo, L. P. Preparation and Electrical Characterization of Polymer Electrolytes: A Review. *Mater. Today: Proc.* **2019**, *17*, 446−458.

(17) Zhao, L.; Fu, J.; Du, Z.; Jia, X.; Qu, Y.; Yu, F.; Du, J.; Chen, Y. High-Strength and Flexible Cellulose/PEG Based Gel Polymer Electrolyte with High Performance for Lithium Ion Batteries. *J. Membr. Sci.* **2020**, *593*, No. 117428.

(18) Zhu, M.; Wu, J.; Wang, Y.; Song, M.; Long, L.; Siyal, S. H.; Yang, X.; Sui, G. Recent Advances in Gel Polymer Electrolyte for High-Performance Lithium Batteries. *J. Energy Chem.* **2019**, *37*, 126−142.

(19) Liu, B.; Huang, Y.; Cao, H.; Zhao, L.; Huang, Y.; Song, A.; Lin, Y.; Li, X.; Wang, M. A Novel Porous Gel Polymer Electrolyte Based on Poly(Acrylonitrile-Polyhedral Oligomeric Silsesquioxane) with High Performances for Lithium-Ion Batteries. *J. Membr. Sci.* **2018**, *545*, 140−149.

(20) Xu, L.; Li, G.; Guan, J.; Wang, L.; Chen, J.; Zheng, J. Garnet-Doped Composite Polymer Electrolyte with High Ionic Conductivity for Dendrite-Free Lithium Batteries. *J. Energy Storage* **2019**, *24*, No. 100767.

(21) Liang, S.; Yan, W.; Wu, X.; Zhang, Y.; Zhu, Y.; Wang, H.; Wu, Y. Gel Polymer Electrolytes for Lithium Ion Batteries: Fabrication, Characterization and Performance. *Solid State Ionics* **2018**, *318*, 2−18.

(22) Xiao, W.; Wang, Z.; Zhang, Y.; Fang, R.; Yuan, Z.; Miao, C.; Yan, X.; Jiang, Y. Enhanced Performance of P(VDF-HFP)-Based Composite Polymer Electrolytes Doped with Organic-Inorganic Hybrid Particles PMMA-ZrO2 for Lithium Ion Batteries. *J. Power Sources* **2018**, *382*, 128−134.

(23) Gregorio, V.; García, N.; Tiemblo, P. Solvent-Free and Scalable Procedure to Prepare PYR13TFSI/LiTFSI/PVDF−HFP Thermoplastic Electrolytes with Controlled Phase Separation and Enhanced Li Ion Diffusion. *Membranes* **2019**, *9*, No. 50.

(24) Jang, S.-H.; Kim, J.-K. Polymer-Ceramic Composite Gel Polymer Electrolyte for High-Electrochemical-Performance Lithium-Ion Batteries. *J. Korean Electrochem. Soc.* **2016**, *19*, 123−128.

(25) Huang, H.; Ding, F.; Zhong, H.; Li, H.; Zhang, W.; Liu, X.; Xu, Q. Nano-SiO 2 -Embedded Poly(Propylene Carbonate)-Based Composite Gel Polymer Electrolyte for Lithium−Sulfur Batteries. *J. Mater. Chem. A* **2018**, *6*, 9539−9549.

(26) Xiao, Q.; Deng, C.; Wang, Q.; Zhang, Q.; Yue, Y.; Ren, S. In Situ Cross-Linked Gel Polymer Electrolyte Membranes with Excellent Thermal Stability for Lithium Ion Batteries. *ACS Omega* **2019**, *4*, 95−103.

(27) Sakakibara, T.; Kitamura, M.; Honma, T.; Kohno, H.; Uno, T.; Kubo, M.; Imanishi, N.; Takeda, Y.; Itoh, T. Cross-Linked Polymer

Electrolyte and Its Application to Lithium Polymer Battery. *Electrochim. Acta* **2019**, *296*, 1018−1026.
(28) An, S. Y.; Jeong, I. C.; Won, M. S.; Jeong, E. D.; Shim, Y. B. Effect of Additives in PEO/PAA/PMAA Composite Solid Polymer Electrolytes on the Ionic Conductivity and Li Ion Battery Performance. *J. Appl. Electrochem.* **2009**, *39*, 1573−1578.
(29) Singh, T. J.; Bhat, S. V. Increased Lithium-Ion Conductivity in (PEG)46LiClO4 Solid Polymer Electrolyte with δ-Al2O3 Nanoparticles. *J. Power Sources* **2004**, *129*, 280−287.
(30) Li, L.; Deng, Y.; Chen, G. Status and Prospect of Garnet/Polymer Solid Composite Electrolytes for All-Solid-State Lithium Batteries. *J. Energy Chem.* **2020**, *50*, 154−177.
(31) Pradeepa, P.; Edwinraj, S.; Ramesh Prabhu, M. Effects of Ceramic Filler in Poly(Vinyl Chloride)/Poly(Ethyl Methacrylate) Based Polymer Blend Electrolytes. *Chin. Chem. Lett.* **2015**, *26*, 1191−1196.
(32) Zhu, P.; Yan, C.; Dirican, M.; Zhu, J.; Zang, J.; Selvan, R. K.; Chung, C.-C.; Jia, H.; Li, Y.; Kiyak, Y.; Wu, N.; Zhang, X. Li 0.33 La 0.557 TiO 3 Ceramic Nanofiber-Enhanced Polyethylene Oxide-Based Composite Polymer Electrolytes for All-Solid-State Lithium Batteries. *J. Mater. Chem. A* **2018**, *6*, 4279−4285.
(33) Wang, X.; Zhang, Y.; Zhang, X.; Liu, T.; Lin, Y. H.; Li, L.; Shen, Y.; Nan, C. W. Lithium-Salt-Rich PEO/Li0.3La0.557TiO3 Interpenetrating Composite Electrolyte with Three-Dimensional Ceramic Nano-Backbone for All-Solid-State Lithium-Ion Batteries. *ACS Appl. Mater. Interfaces* **2018**, *10*, 24791−24798.
(34) Cha, J. H.; Didwal, P. N.; Kim, J. M.; Chang, D. R.; Park, C.-J. Poly(Ethylene Oxide)-Based Composite Solid Polymer Electrolyte Containing Li7La3Zr2O12 and Poly(Ethylene Glycol) Dimethyl Ether. *J. Membr. Sci.* **2020**, *595*, No. 117538.
(35) Zhu, L.; Zhu, P.; Yao, S.; Shen, X.; Tu, F. High-Performance Solid PEO/PPC/LLTO-Nanowires Polymer Composite Electrolyte for Solid-State Lithium Battery. *Int. J. Energy Res.* **2019**, *43*, 4854−4866.
(36) Chen, T.; Kong, W.; Zhang, Z.; Wang, L.; Hu, Y.; Zhu, G.; Chen, R.; Ma, L.; Yan, W.; Wang, Y.; Liu, J.; Jin, Z. Ionic Liquid-Immobilized Polymer Gel Electrolyte with Self-Healing Capability, High Ionic Conductivity and Heat Resistance for Dendrite-Free Lithium Metal Batteries. *Nano Energy* **2018**, *54*, 17−25.
(37) Anuar, N. K.; Subban, R. H. Y.; Mohamed, N. S. Properties of PEMA-NH4CF3SO3 Added to BMATSFI Ionic Liquid. *Materials* **2012**, *5*, 2609−2620.
(38) Philip, P.; Tomlal Jose, E.; Chacko, J. K.; Philip, K. C.; Thomas, P. C. Preparation and Characterisation of Surface Roughened PMMA Electrospun Nanofibers from PEO - PMMA Polymer Blend Nanofibers. *Polym. Test.* **2019**, *74*, 257−265.
(39) Li, B.; Su, Q.; Yu, L.; Wang, D.; Ding, S.; Zhang, M.; Du, G.; Xu, B. Li 0.35 La 0.55 TiO 3 Nanofibers Enhanced Poly(Vinylidene Fluoride)-Based Composite Polymer Electrolytes for All-Solid-State Batteries. *ACS Appl. Mater. Interfaces* **2019**, *11*, 42206−42213.
(40) Wang, P.; Xu, P.; Zhou, Y.; Yang, Y.; Ding, Y. Effect of MWCNTs and P[MMA-IL] on the Crystallization and Dielectric Behavior of PVDF Composites. *Eur. Polym. J.* **2018**, *99*, 58−64.
(41) Lim, Y.; Jung, H.-A.; Hwang, H. Fabrication of PEO-PMMA-LiClO4-Based Solid Polymer Electrolytes Containing Silica Aerogel Particles for All-Solid-State Lithium Batteries. *Energies* **2018**, *11*, 2559.
(42) Chen, X.; Xie, Y.; Ling, Y.; Zhao, J.; Xu, Y.; Tong, Y.; Li, S.; Wang, Y. Ionic Liquid Crystal Induced Morphological Control of Solid Composite Polymer Electrolyte for Lithium-Ion Batteries. *Mater. Des.* **2020**, *192*, No. 108760.
(43) He, K.; Zha, J.; Du, P.; Cheng, S. H.; Liu, C.; Dang, Z.; Li, R. K. Y. Tailored High Cycling Performance in a Solid Polymer Electrolyte with Perovskite-Type Li0.33La0.557TiO3 Nanofibers for All-Solid-State Lithium Ion Batteries. *Dalton Trans.* **2019**, *48*, 3263−3269.


https://doi.org/10.1021/acsomega.1c03140
*ACS Omega* 2021, 6, 25329−25337